

The British University in Egypt

BUE Scholar

Nanotechnology Research Centre

Research Centres

8-3-2022

Modeling the electronic properties for CNT interacted with ZnO, CuO, and Co₃O₄

Mohamed Morsy

mohamed.morsy@bue.edu.eg

Follow this and additional works at: https://buescholar.bue.edu.eg/nanotech_research_centre



Part of the [Condensed Matter Physics Commons](#)

Recommended Citation

Morsy, Mohamed, "Modeling the electronic properties for CNT interacted with ZnO, CuO, and Co₃O₄" (2022). *Nanotechnology Research Centre*. 26.

https://buescholar.bue.edu.eg/nanotech_research_centre/26

This Article is brought to you for free and open access by the Research Centres at BUE Scholar. It has been accepted for inclusion in Nanotechnology Research Centre by an authorized administrator of BUE Scholar. For more information, please contact bue.scholar@gmail.com.



Modeling the electronic properties for CNT interacted with ZnO, CuO, and Co₃O₄

Walaa M. Taha¹ · Mohamed Morsy^{2,4} · Nadra A. Nada¹ · Medhat A. Ibrahim^{3,4}

Received: 27 July 2021 / Accepted: 7 July 2022
© The Author(s) 2022

Abstract

Because of the wide applications of carbon nanotubes (CNTs) and magic properties of metal oxides, Hartree–Fock quantum mechanical calculations at HF/STO-3G were applied to study the electronic properties of CNTs and their interaction with ZnO, CuO, and Co₃O₄. Calculations were conducted to calculate HOMO/LUMO bandgap energy ΔE , molecular electrostatic potential (MESP), and total dipole moment (TDM) for CNTs, CNT-Zn-O, CNT-Cu-O, CNT-Co-O, and CNT-O-Zn, CNT-O-Cu, CNT-O-Co following the two mechanisms of interaction as adsorbed and complex state. The calculations show that the interaction of CNTs with metal oxides increases its reactivity where MESP indicated to more distribution charges and an increase in the TDM value after the interaction of CNTs with metal oxides. Where the interaction of CNT-Co-O as adsorbed state has the highest TDM with the lowest bandgap ΔE which confirms that CNT-Co₃O₄ can be used in sensing devices.

Keywords HF/STO-3G · CNTs · Metal oxides · HOMO/LUMO bandgap energy · MESP · TDM

1 Introduction

Since the discovery of CNTs by Iijima (1991), the subject takes great attention in scientific research due to it is logical electronic physical, and mechanical properties. Where, large surface area, high thermal and electrical conductivity of CNTs make them applicable in several fields of energy storage devices such as solar cells, supercapacitors, and sensors applications

✉ Medhat A. Ibrahim
medahmed6@yahoo.com

¹ Physics Department, Faculty of Women for Arts, Science and Education, Ain Shams University, Cairo 11757, Egypt

² Building Physics and Environment Institute, Housing & Building National Research Center (HBRC), Dokki, Giza 12311, Egypt

³ Molecular Spectroscopy and Modeling Unit, National Research Centre, 35 El-Behouth St., Dokki, Giza 12622, Egypt

⁴ Nanotechnology Research Center (NTRC), The British University in Egypt, Suez Desert Road, El-Sherouk City, Cairo 11837, Egypt

(Smalley 2003; Scoville et al. 1991; Habila et al. 2017; Kamas et al. 2021). There are two main types of CNTs the first is a single-wall carbon nanotube (SWCNT) which is considered as a graphene sheet rolled up to form a single cylinder in a nanoscale. While the second type is called multiwall carbon nanotubes (MWCNT) which are several multilayers of concentric tubes (Klump et al. 2006; Erik et al. 2017; Soylak and Unsal 2009). Synthesizing process of CNTs is achieved by different methods. The most important and well-known methods are arc discharge, laser ablation, and chemical vapor deposition (CVD) (Awasthi et al. 2005; Isaacs et al. 2010). Functionalization of CNTs enhances its physical properties and takes nanotubes to a very wide range of applications (Morsy et al. 2015; Ytreberg et al. 2017). It must be covalent or noncovalent functionalizations. Covalent functionalization causes change hybridization from SP₂ to SP₃ and noncovalent such as van der Waal's force i.e. adsorption of atoms or small molecules on the outer surface of CNTs (Hirsch and Vostrowsky 2005). While noncovalent interaction and functionalization are preferred because it conserves electrical properties and does not disturb π electrons delocalization (Speranza 2019). In recent years the semiconductor metal oxides have great attention due to their magical properties of high stability, chemical, physical, electronic, and high responsibility for sensor applications (Chavali and Nikolova 2019). Researchers found that the combination between CNTs and metal oxides nanoparticles improves the sensor's responsibility (Korotcenkov and Cho 2017).

Molecular modeling is useful to understand the electronic structure, chemical and physical properties of many molecules, where the computational work attaches and simplifies the communication between theoretical and experimental results. Molecular modeling is divided into two branches, the first is called molecular mechanics which predicts the structure of molecule applying the classical physics and studies the interactions that act upon nuclei. The second one is the electronic structure methods that are solving Schrodinger equations. Electronic structure methods are divided into two classes which are semi-empirical methods and Ab initio methods. Solving the Schrodinger equation, total energy and TDM can be obtained from the first derivative of the Schrodinger equation while the vibration frequency appears in Raman and IR spectroscopy in addition to other physical parameters are obtained from the second derivative (Foresman and Frisch 1996).

Recently researchers are applying molecular modeling to understand the structural properties of carbon nanomaterials (Ezzat et al. 2018, 2020; Elhaes et al. 2018). Zollo and Gala (2012) studied the structure of carbon nanomaterials with various atomizing methods of gas adsorption one of these methods is HF method, where the interaction configuration in the ground state is replaced by a linear combination state and the excited state is replaced by virtual molecular orbitals (Young 2001).

The interactions of CNTs with metal oxides and the effect of functionalization on the surface of CNTs are explained by molecular modeling where the effect of functionalization is very important for certain well applications.

The present work aimed to study CNT and CNT interacted with ZnO, CuO, and Co₃O₄ following the two mechanisms of interaction: adsorb and complex states. The electronic properties were studied in terms of calculated TDM, HOMO–LUMO bandgap energy, and MESP at the HF/ STO-3G level of theory.

2 Calculations details

All calculations were carried out using Gaussian 09 program (Frisch et al. 2010) at Spectroscopy Department, National Research Centre (NRC), Cairo, Egypt. Model molecules were subjected to optimization using HF method at STO-3G basis set (Stewart 1970). Then, three physical parameters namely HOMO/LUMO molecular orbital, TDM, and MESP were calculated for all studied structures at the same level of theory.

3 Results and discussion

3.1 Building the model molecules

A model molecule was designed to form the structure of CNT. This CNT is formed by rolling graphene sheet to obtain a hollow cylinder consisting of hexagonal carbon rings of 84 carbon atoms. As shown in Fig. 1 some modifications act on the surface of CNT throughout the interaction of CNT with different metal oxides like CNT-Zn-O, CNT-Cu-O, and CNT-Co-O at the same carbon atom. Figure 2 described the model structures for the interaction of CNT with metal oxides throughout the oxygen as CNT-O-Zn, CNT-O-Cu, CNT-O-Co as adsorb state. There is also another interaction mechanism that can be studied which is the complex interaction. In this case the CNT can interact with ZnO, CuO, and Co_3O_4 as a complex interaction. Also, this interaction can be processed throughout the metal atom as shown in Fig. 3 and throughout the oxygen atom as presented in Fig. 4.

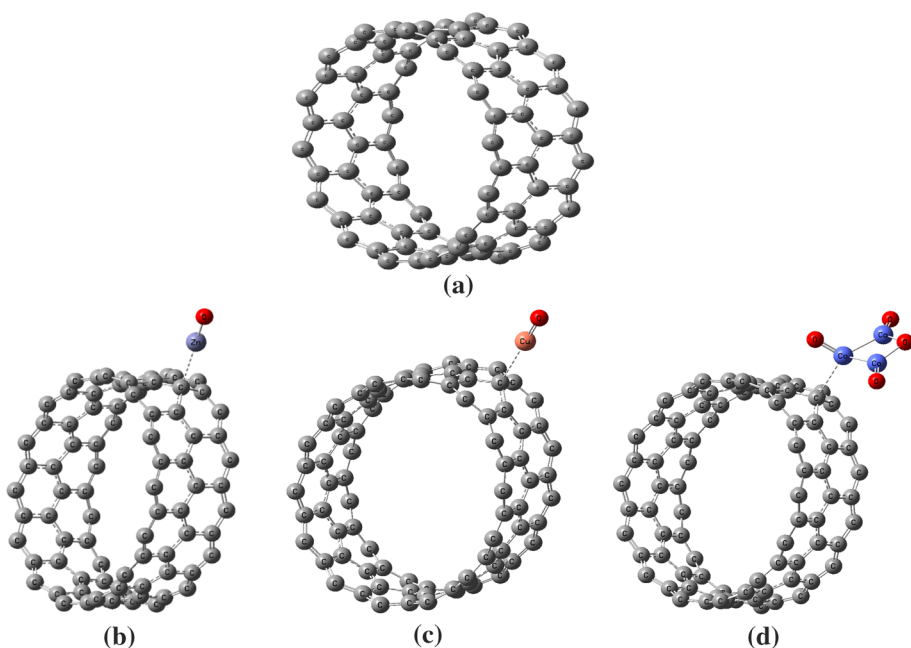


Fig. 1 Model structure for **a** CNT, **b** CNT-Zn-O, **c** Cu-O, and **d** Co-O as adsorb state

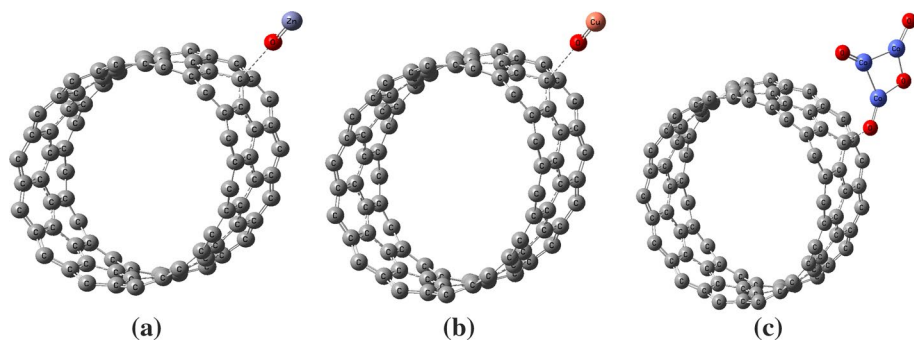


Fig. 2 Model structure for **a** CNT-O-Zn, **b** CNT-O-Cu and **c** CNT-O-Co as adsorb state

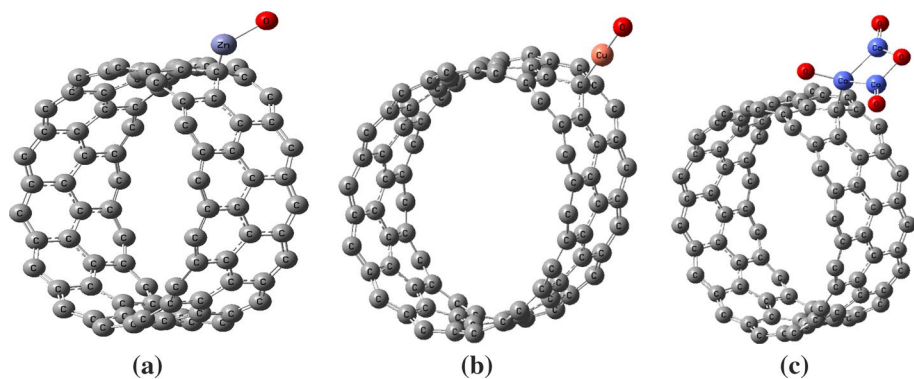


Fig. 3 Model structure for **a** CNT-Zn-O, **b** CNT-Cu-O, and **c** CNT-Co-O as a complex state

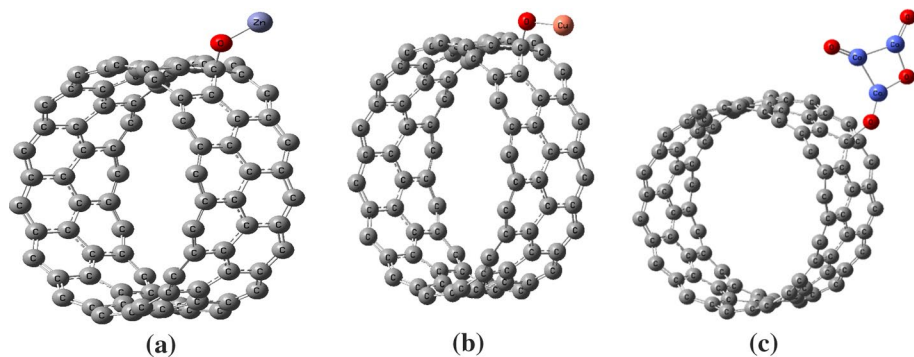


Fig. 4 Model structure for **a** CNT-O-Zn, **b** CNT-O-Cu, and **c** CNT-O-Co as a complex state

3.2 HOMO/LUMO and MESP for CNT

HOMO and LUMO are the most important orbitals in the molecule where HOMO is the highest occupied molecular orbital and LUMO is the lowest unoccupied molecular orbital.

The difference in energy between the HOMO and LUMO orbitals gives the bandgap energy where the most excitations occur. HOMO/LUMO band gap calculations are useful to study the electrical properties of the studied structures. MESP is an important parameter to describe the nucleophilic and electrophilic active sites of CNT structure and for CNT interacted with metal oxides. Generally, MESP measures the interactions of charges around the surface. Mapping MESP contours on the surface of the nanotube enable us how to activate the CNT surface by illustrating the distribution of charges on the surface of CNT by following a color mapping. The potential is high at red color then followed decrease until blue color to red > orange > yellow > green than blue then blue > blue (Murray and Sen 1996; Şahin et al. 2015).

Figure 5 presented the HOMO/LUMO and MESP for CNT. Firstly, the HOMO and LUMO molecular orbitals are distributed along the surface of CNT. MESP for CNT showed that only yellow color appears refers to the uniform distribution of charges inside and outside the surface of CNT ascribed no changing in the electronegativity. Therefore, it is important to study the interaction of CNT with metal oxides to manipulate its reactivity properties.

3.2.1 HOMO/LUMO and MESP for CNT-metal oxides as adsorb state

Figure 6 displayed HOMO–LUMO orbitals for CNT-Zn-O, CNT-Cu-O, and CNT-Co-O as adsorb state. Figure 6a described HOMO/LUMO orbitals distribution in case of interactions of CNT with Zn-O which are approximately the same distributions of CNT structure Fig. 5a. As shown in Fig. 6b. HOMO/LUMO orbitals of CNT interacted with Cu-O localized far away from the Cu-O. While for CNT interact with Co-O, the orbitals distributed around the metal oxide from right and left as shown in Fig. 6c. Figure 7 showed the calculated MESP for CNT-Zn-O, CNT-Cu-O and CNT-Co-O as adsorb state. There are color changes from red to blue color in the three structures toward the metal oxides position. Such colors indicated to the active sites at the surface of CNT interacted with the three metal oxides individually. The results confirm the same obtained before (Politzer et al. 1986). Therefore, mapping colors demonstrated that the adsorption of metal oxides on the surface of nanotubes manipulates the reactivity of CNT and direct functionalized CNT toward a wide range of applications.

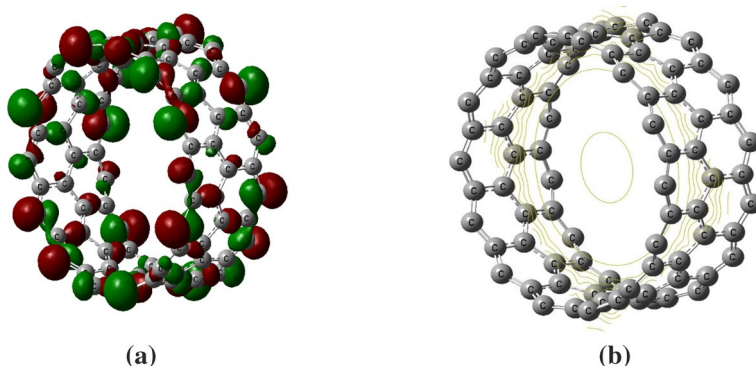


Fig. 5 HF/STO-3G calculated **a** HOMO/LUMO for CNT and **b** MESP for the CNT model

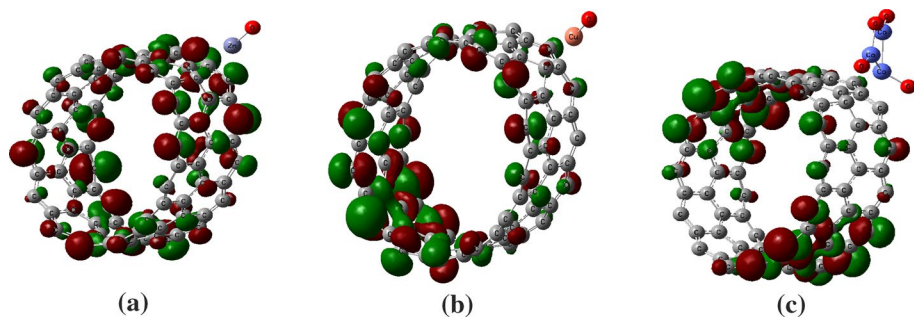


Fig. 6 HF/STO-3G calculated HOMO/LUMO orbitals for adsorbed: **a** CNT-Zn-O, **b** CNT-Cu-O and **c** CNT-Co-O as adsorb state

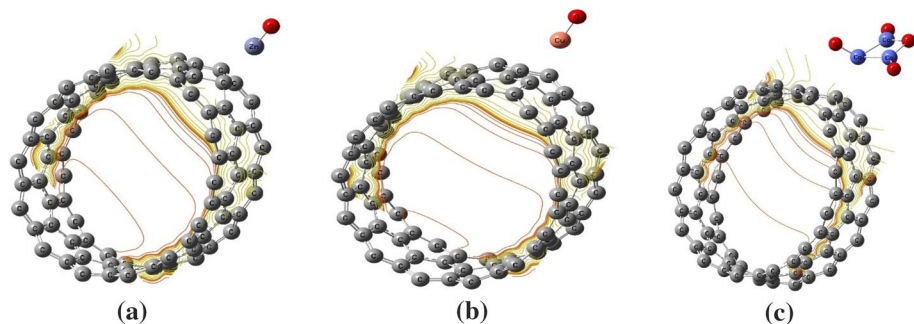


Fig. 7 HF/STO-3G calculated MESP as contour for **a** CNT-Zn-O, **b** CNT-Cu-O and **c** CNT-Co-O as adsorb state

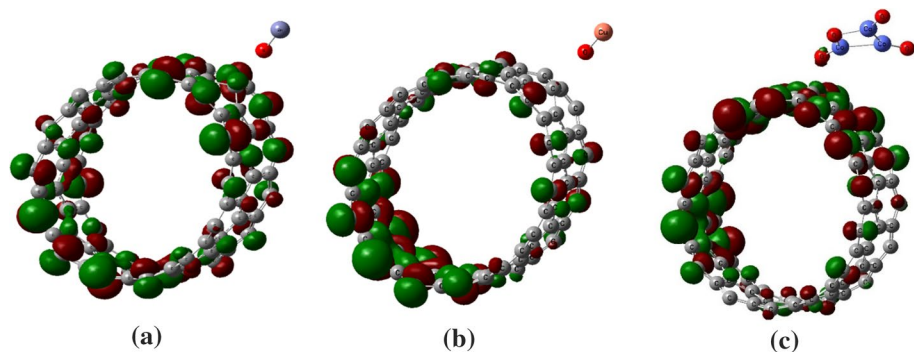


Fig. 8 HF/STO-3G calculated HOMO/LUMO orbitals for adsorbed: **a** CNT-O-Zn **b** CNT-O-Cu **c** CNT-O-Co

For the interaction of CNT-O-Zn, CNT-O-Cu, and CNT-O-Co, the same calculations are applied at the same carbon atom as adsorb state. HOMO/LUMO orbitals and MESP are also calculated as presented in Figs. 8 and 9 respectively. MESP maps displayed the electronegativity of CNT increased because of the interaction of CNT with the different metal oxides through the oxygen atom. The red color appears around the structures represented

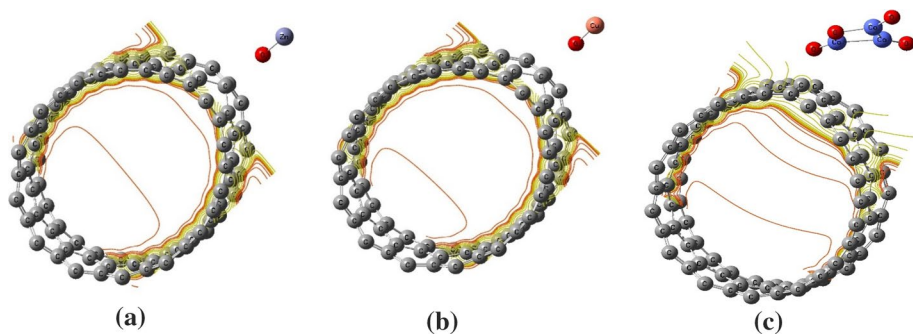


Fig. 9 HF/STO-3G calculated MESP as contour for adsorbed: **a** CNT-O-Zn **b** CNT-O-Cu **c** CNT-O-Co

CNT-O-metal unlike the mapping of MESP of CNT structure. The results confirm that the CNT became more reactive due to the interaction with metal oxides. Also, Fig. 9 showed that the reactivity of CNT-O-Co model molecule is higher than that of the other models as the intensity of the red color increased within the structure. Meanwhile, there are more charges transferred on the CNT surface when the interaction is processed via the oxygen atom.

3.2.2 HOMO/LUMO and MESP for CNT-metal oxides as a complex

HOMO/LUMO orbitals and MESP calculations revealed an observed difference between the two mechanisms of interaction between CNT and metal oxides when the interaction is complex. Figure 10a–c present the HOMO/LUMO molecular orbitals of CNT complexed with Zn-O, Cu-O, and with Co-O respectively. MESP maps are presented in Fig. 10d–f for complex CNT-Zn-O, CNT-Cu-O, and CNT-Co-O respectively. It is clear from the figures that the intensity of red color is nearly identical for the three structures but, it is still less than that observed within the adsorbed structures of CNT-Zn-O, CNT-Cu-O, and CNT-Co-O. Meanwhile, Fig. 11a–c showed the HOMO/LUMO orbitals of CNT-O-Zn, CNT-O-Cu, and CNT-O-Co as complex state respectively. The figures showed that the distribution of electrons within the orbitals for CNT complexed with Cu-O is identical to that complexed with O-Cu. In contrast, for CNT-O-Zn and CNT-O-Co, the electrons distribution within the HOMO/LUMO orbitals differs from that for CNT-Zn-O and CNT-Co-O as complex. While Fig. 11d–f showed the MESP for complexed CNT interacted with the three metal oxides under study through the oxygen atom. Similarly, for the complex interactions processed through the oxygen atom, the red color is distributed equally within the models representing CNT-O-Zn, CNT-O-Cu, and CNT-O-Co. As presented in Figs. 9a–c and 11d–f, it is clear that the electronegativity for the adsorbed interaction processed through oxygen is higher than that for the complex interaction. This means that the reactivity of the oxygenated adsorbed interaction is higher than that of the complexed one.

3.3 TDM and energy gap ΔE calculation for CNT-metal oxides as adsorb

The reactive property of CNT structure and the interaction of CNT with metal oxides is determined by the two physical parameters: total dipole moment (TDM) and ΔE value. Where the reactivity increased when the TDM increased, and the ΔE decreased. The

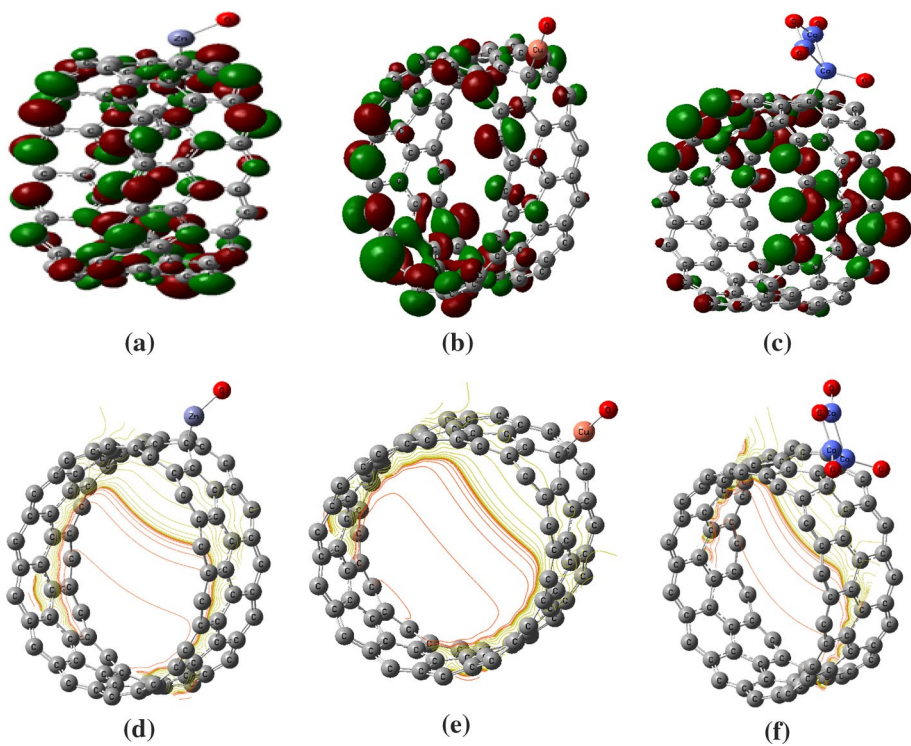


Fig. 10 HF/STO-3G calculated HOMO/LUMO orbitals for **a** CNT-Zn-O, **b** CNT-Cu-O, and **c** CNT-Co-O and MESP as contour for **d** CNT-Zn-O, **e** CNT-Cu-O and **f** CNT-Co-O as complex

minimum ΔE means that the material becomes more conducting and subsequently increases interactions around the surface (Bayoumy et al. 2020). Table 1 presents the values of both TDM and ΔE for CNT and its interaction with metal oxides as adsorb state where the interaction is processed through the metal atom. The calculated TDM of CNT is 0.43 Debye while, the ΔE value is 1.94 eV. As a result of interaction with metal oxides, TDM value became: 3.62, 12.35, and 21.1 Debye for CNT-Zn-O, CNT-Cu-O, and CNT-Co-O respectively. However, as presented in the table, the bandgap energy increased as a result of interaction with the different metal oxides. Where, it takes values 4.45, 3.51, and 2.66 eV for CNT-Zn-O, CNT-Cu-O, and CNT-Co-O respectively. The results indicated that CNT-Co-O has the highest TDM with the lowest bandgap energy compared with CNT-Cu-O and then CNT-Zn-O.

Regarding the TDM and ΔE for CNT-O-metals as adsorb state, Table 2 presents the TDM and bandgap energy of CNT-O-Zn, CNT-O-Cu, and CNT-O-Co as adsorbed state. For CNT interacted with O-Zn and O-Cu, TDM equals 5.38 and 1.00 Debye while ΔE equals 4.21 and 5.60 eV, respectively. Meanwhile, TDM and bandgap energy equal 1.37 Debye and 6.61 eV for CNT interact with O-Co. These results indicated that the composite CNT-O-Zn has the highest TDM with the lowest ΔE and prove that CNT-O-Zn is higher reactive than CNT-O-Co and CNT-O-Cu. Comparing the results of Tables 1 and 2, it is concluded that the interaction between CNT and the different metal oxides is often adsorbed. Where, the CNT-Zn-O, CNT-Cu-O, and CNT-Co-O studied structures

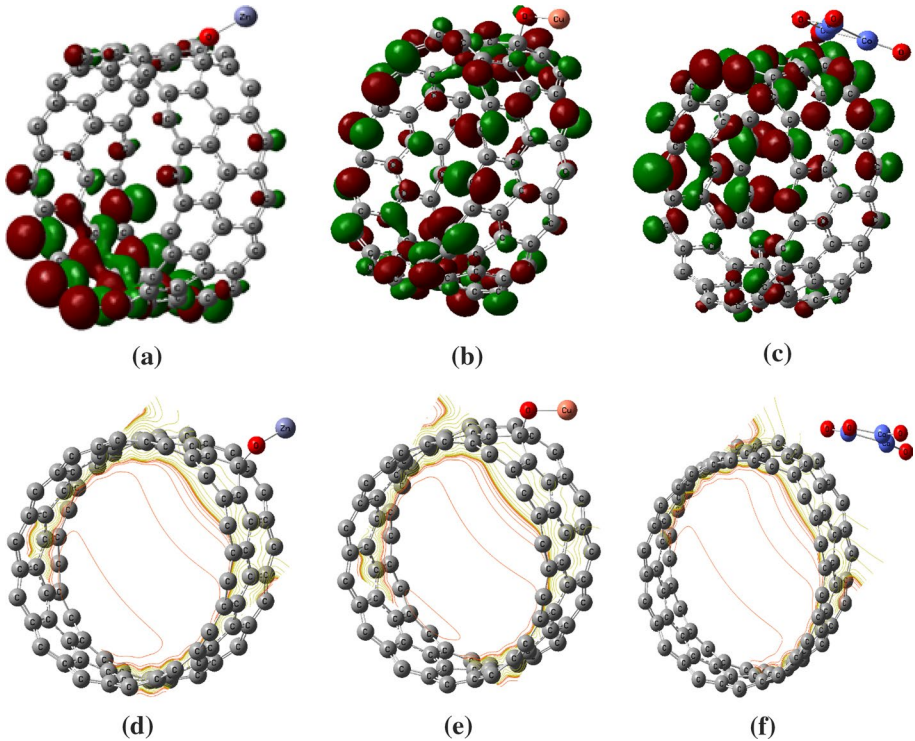


Fig. 11 HF/STO-3G calculated HOMO/LUMO orbitals for **a** CNT-O-Zn, **b** CNT-O-Cu, and **c** CNT-O-Co and MESP as contour for **d** CNT-O-Zn, **e** CNT-O-Cu and **f** CNT-O-Co as complex

Table 1 HF/STO-3G calculated TDM as (Debye) and HOMO/LUMO band gap energy (ΔE) as (eV) for CNT and CNT-Zn-O, CNT-Cu-O, and CNT-Co-O as adsorb state

Structure	TDM (Debye)	ΔE (eV)
CNT	0.43	1.94
CNT-Zn-O	3.62	4.45
CNT-Cu-O	12.35	3.51
CNT-Co-O	21.1	2.66

Table 2 HF/STO-3G calculated TDM as (Debye) and HOMO/LUMO band gap energy (ΔE) as (eV) for CNT-O-Zn, CNT-O-Cu, and CNT-O-Co as adsorb

Structure	TDM (Debye)	ΔE (eV)
CNT-O-Zn	5.38	4.21
CNT-O-Cu	1.00	5.60
CNT-O-Co	1.37	6.61

possess the highest TDM and lowest bandgap values when the interaction is supposed to be adsorbed. The results of TDM and ΔE confirm the MESP results that the model molecule represents CNT-Co-O is the most reactive one. Additionally, this result confirms that the CNT-Co-O model molecule can be used in sensing devices.

Table 3 HF/STO-3G calculated TDM as (Debye) and HOMO/LUMO band gap energy (ΔE) as (eV) for CNT-Zn-O, CNT-Cu-O, and CNT-Co-O as complex

Structure	TDM (Debye)	ΔE (eV)
CNT-Zn-O	4.43	4.54
CNT-Cu-O	0.81	5.75
CNT-Co-O	13.91	4.81

Table 4 HF/STO-3G calculated TDM as (Debye) and HOMO/LUMO band gap energy (ΔE) as (eV) for CNT-O-Zn, CNT-O-Cu, and CNT-O-Co as complex

Structure	TDM (Debye)	ΔE (eV)
CNT-O-Zn	19.76	3.84
CNT-O-Cu	3.38	5.36
CNT-O-Co	1.37	6.61

3.3.1 TDM and ΔE calculation for CNT-metal oxides as complex state

For CNT-Metal-O interaction, Table 3 presents the calculated TDM and ΔE for CNT-Zn-O, CNT-Cu-O, and CNT-Co-O as complex state. Where TDM equals 4.43, 0.81, and 13.91 Debye for CNT-Zn-O, CNT-Cu-O, and CNT-Co-O, respectively. Meanwhile, the ΔE takes values of 4.54, 5.75, and 4.81 eV for the same sequence. The obtained results confirmed that the reactivity of the CNT-Co-O model molecule is higher than that of CNT-Zn-O and CNT-Cu-O because of the highest TDM. However, TDM and HOMO/LUMO energy for complexed CNT-O-Zn, CNT-O-Cu, and CNT-O-Co are tabulated in Table 4. Where, its values are 19.79, 3.38, and 1.37 Debye and 3.84, 5.36, and 6.61 eV, respectively for CNT-O-Zn, CNT-O-Cu, and CNT-O-Co. This result deduced the structure of CNT-O-Zn and CNT-O-Cu are more reactive than that processed through the metal atom in contrast CNT-O-Co structure.

Finally, as shown in Table 4 the interaction of ZnO from oxygen atom as complex differs from the expected result. This is because the ZnO is an n-type semiconductor where the valance band is related to the 2p level in oxygen and the conduction bands come from the 4s level of zinc atom, electrons move from valance bands to conduction bands leaving holes in the valance band (Li et al. 2020; Harun et al. 2016). Therefore in case of the strong interaction between CNT and ZnO, holes directed to transfer between Oxygen to CNT introduced positive charge transfer around the CNT surface. This charge transfer enhanced the reactivity of the composite surface (Gupta and Saleh 2011; Boscarino et al. 2019).

4 Conclusion

The interaction between CNT and Zn, CuO, and Co₃O₄ nanoparticles was subjected to quantum mechanical calculations. HF/STO-3G method is suitable for studying the molecular structure of CNT and the interaction of CNT with ZnO, CuO, and Co₃O₄. The TDM value, ΔE , and MEP are studied at the same level of theory. The mechanism of the interaction between CNT and nano metal oxides was studied as a complex state and adsorbed state. The MESP studies showed the distribution of charges and the presence of electrophilic-nucleophilic charges in the interaction between CNT and metal oxides in

comparison with CNT that is neutral. This indicates that the interaction of CNT with metal oxides enhances its reactivity. Also, results of calculated TDM confirm the MESP results, where TDM of CNT increased due to the interaction of CNT with metal oxides. The results showed that the highest reactivity and highest TDM belong to CNT-Co-O as adsorb state because of the more vacancies present in cobalt oxide. Additionally, ΔE results showed that CNT-Co-O as adsorb state has the lowest value of ΔE and the most reactive one in comparison with the other structures. This makes CNT-Co-O suitable for application as a sensor. The results confirm also that the adsorption state is better than complex state when interacting through metal atom.

Funding Open access funding provided by The Science, Technology & Innovation Funding Authority (STDF) in cooperation with The Egyptian Knowledge Bank (EKB). The authors have not disclosed any funding.

Declarations

Conflict of interest The authors have not disclosed any competing interests.

Open Access This article is licensed under a Creative Commons Attribution 4.0 International License, which permits use, sharing, adaptation, distribution and reproduction in any medium or format, as long as you give appropriate credit to the original author(s) and the source, provide a link to the Creative Commons licence, and indicate if changes were made. The images or other third party material in this article are included in the article's Creative Commons licence, unless indicated otherwise in a credit line to the material. If material is not included in the article's Creative Commons licence and your intended use is not permitted by statutory regulation or exceeds the permitted use, you will need to obtain permission directly from the copyright holder. To view a copy of this licence, visit <http://creativecommons.org/licenses/by/4.0/>.

References

- Awasthi, K., Srivastava, A., Srivastava, O.N.: Synthesis of carbon nanotubes. *J. Nanosci. Nanotechnol.* **5**(10), 1616–1636 (2005). <https://doi.org/10.1166/jnn.2005.407>
- Bayoumy, A.M., Refaat, A., Yahia, I.S., Zahran, H.Y., Elhaes, H., Ibrahim, M.A., Shkir, M.: Functionalization of graphene quantum dots (GQDs) with chitosan biopolymer for biophysical applications. *Opt. Quantum Electron.* **52**, 16 (2020). <https://doi.org/10.1007/s11082-019-2134-z>
- Boscarino, S., Filice, S., Sciuto, A., Libertino, S., Scuderi, M., Galati, C., Scalese, S.: Investigation of ZnO-decorated CNTs for UV light detection applications. *Nanomaterials* **9**(8), 1099 (2019). <https://doi.org/10.3390/nano9081099>
- Chavali, M.S., Nikolova, M.P.: Metal oxide nanoparticles and their applications in nanotechnology. *SN Appl. Sci.* **607** (2019). <https://doi.org/10.1007/s42452-019-0592-3>
- Elhaes, H., Ezzat, H., Badry, R., Yahia, I.S., Zahran, H.Y., Ibrahim, M.A.: The interaction between carbon nanotube decorated with CuO and ZnO and hydrogen. *Sensor Lett.* (2018). <https://doi.org/10.1166/sl.2018.3969>
- Ezzat, H., Ibrahim, M., Elhaes, H.: Molecular modeling applied for carbon nano materials. *Egypt J. Chem.* **63**(12), 4777–4787 (2020). <https://doi.org/10.21608/EJCHEM.2020.26861.2551>
- Ezzat, H., Badry, R., Yahia, I.S., Zahran, H.Y., Elhaes, H., Ibrahim, M.A.: Mapping the molecular electrostatic potential of carbon nanotubes. *Biointerface Res. Appl.* **8**, 3539–3542 (2018)
- Foresman, J.B., Frisch, E.: *Exploring Chemistry with Electronic Structure Methods*. Gaussian Inc., Pittsburgh (1996)
- Frisch, M., Trucks, G., Schlegel, H., Scuseria, G., Robb, M., Cheeseman, J., Scalmani, G., Barone, V., Mennucci, B., Petersson, G., Nakatsuji, H., Caricato, M., Li, X., Hratchian, H., Izmaylov, A., Bloino, J., Zheng, G., Sonnenberg, J., Hada, M., Ehara, M., Toyota, K., Fukuda, R., Hasegawa, J., Ishida, M., Nakajima, T., Honda, Y., Kitao, O., Nakai, H., Vreven, T., Montgomery, J., Jr., Peralta, J., Ogliaro, F., Bearpark, M., Heyd, J., Brothers, E., Kudin, K., Staroverov, V., Keith, T., Kobayashi, R., Normand, J., Raghavachari, K., Rendell, A., Burant, J., Iyengar, S., Tomasi, J., Cossi, M., Rega, N., Millam,

- J., Klene, M., Knox, J., Cross, J., Bakken, V., Adamo, C., Jaramillo, J., Gomperts, R., Stratmann, R., Yazyev, O., Austin, A., Cammi, R., Pomelli, C., Ochterski, J., Martin, R., Morokuma, K., Zakrzewski, V., Voth, G., Salvador, P., Dannenberg, J., Dapprich, S., Daniels, A., Farkas, O., Foresman, J., Ortiz, J., Cioslowski, J., Fox, D.: Gaussian 09 Revision C.01. Gaussian Inc., Wallingford CT (2010)
- Gupta, V., Saleh, T.A.: Syntheses of carbon nanotube-metal oxides composites: adsorption and photo-degradation. In: Carbon Nanotubes-From Research to Applications, pp. 295–312. InTech Croatia, European Union (2011)
- Habila, M.A., Yilmaz, E., AlOthman, Z.A., Soylak, M.: 1-nitroso-2-naphthol impregnated multiwalled carbon nanotubes (NNMWCNTs) for the separation-enrichment and flame atomic absorption spectrometric detection of copper and lead in hair, water, and food samples. *Desalination Water Treat.* **8**, 285–291 (2017). <https://doi.org/10.5004/dwt.2017.21296>
- Harun, K., Mansor, N., Ahmad, Z.A., Mohamad, A.A.: Electronic properties of ZnO nanoparticles synthesized by Sol-gel method: a LDA+ U calculation and experimental study. *Procedia Chem.* **19**, 125–132 (2016). <https://doi.org/10.1016/j.proche.2016.03.125>
- Hirsch, A., Vostrowsky, O.: Functionalization of carbon nanotubes. In: Dieter Schlüter, A. (ed.) *Functional Molecular Nanostructures*, pp. 193–237. Springer, Berlin (2005)
- Iijima, S.: Helical microtubules of graphitic carbon. *Nature* **354**, 56–58 (1991). <https://doi.org/10.1038/354056a0>
- Isaacs, J.A., Tanwani, A., Healy, M.L., Dahlben, L.J.: Economic assessment of single-walled carbon nanotube processes. *J. Nanoparticle Res.* **12**, 551e62 (2010). <https://doi.org/10.1007/s11051-009-9673-3>
- Kamas, D., Karatepe, A., Soylak, M.: Vortex-assisted magnetic solid phase extraction of Pb and Cu in some herb samples on magnetic multiwalled carbon nanotubes. *Turk. J. Chem.* **45**(1), 210–218 (2021). <https://doi.org/10.3906/kim-2009-26>
- Klumpp, C., Kostarelos, K., Prato, M., Bianco, A.: Functionalized carbon nanotubes as emerging nanovectors for the delivery of therapeutics. *Biochim. Biophys. Acta.* **1758**(3), 404–412 (2006). <https://doi.org/10.1016/j.bbame.2005.10.008>
- Korotcenkov, G., Cho, B.K.: Metal oxide composites in conductometric gas sensors: achievements and challenges. *Sens. Actuators B Chem.* **244**, 182–210 (2017). <https://doi.org/10.1016/j.snb.2016.12.117>
- Li, Y., Liao, C., Tjong, S.C.: Recent advances in zinc oxide nanostructures with antimicrobial activities. *Int. J. Mol. Sci.* (2020). <https://doi.org/10.3390/ijms21228836>
- Morsy, M., Helal, M., El-Okr, M., Ibrahim, M.A.: Preparation and characterization of multiwall carbon nanotubes decorated with zinc oxide. *Der Pharma Chem.* **7**(10), 139–144 (2015)
- Murray, J.S., Sen, K.: *Molecular Electrostatic Potentials: Concepts and Applications*. Elsevier, Amsterdam (1996)
- Politzer, P., Laurence, P.R., Jayasuriya, K.: Molecular electrostatic potentials: an effective tool for the elucidation of biochemical phenomena. *Environ. Health Perspect.* (1986). <https://doi.org/10.1289/ehp.8561191>
- Şahin, Z.S., Şenöz, H.I., Tezcan, H., Büyükgüngör, O.: Synthesis, spectral analysis, structural elucidation and quantum chemical studies of (E)-methyl-4-[(2-phenylhydrazono) methyl] benzoate *Spectrochim. Acta A* **143**(15), 91–100 (2015). <https://doi.org/10.1016/j.saa.2015.02.032>
- Scoville, C., Cole, R., Hogg, J., Farooque, O., Russell, A.: Carbon Nanotubes. Notes Lecture 1–11 (1991)
- Smalley, R.E.: *Carbon Nanotubes: Synthesis, Structure, Properties, and Applications*. Springer, Berlin (2003)
- Soylak, M., Unsal, Y.E.: Simultaneous enrichment-separation of metal ions from environmental samples by solid-phase extraction using double-walled carbon nanotubes. *J. AOAC Int.* **92**(4), 1219–1224 (2009). <https://doi.org/10.1093/jaoac/92.4.1219>
- Speranza, G.: The role of functionalization in the applications of carbon materials: an overview *C. J. Carbon Res.* **5**(4), 84 (2019). <https://doi.org/10.3390/c5040084>
- Stewart, R.F.: Small Gaussian expansions of Slater-type orbitals. *J. Chem. Phys.* **52**(1), 431–438 (1970). <https://doi.org/10.1063/1.1672702>
- Young, D.C.: *A Practical Guide for Applying Techniques to Real-World Problems*. Wiley, New York (2001)
- Ytreberg, E., Lagerström, M., Holmqvist, A., Eklund, B., Elwing, H., Dahlström, M., Dahl, P., Dahlström, M.: A novel XRF method to measure environmental release of copper and zinc from antifouling paints. *Environ. Pollut.* **225**(1), 490–496 (2017). <https://doi.org/10.1016/j.envpol.2017.03.014>
- Zollo, G., Gala, F.: Atomistic modeling of gas adsorption in nanocarbons. *J. Nanomater.* (2012). <https://doi.org/10.1155/2012/152489>